Contents lists available at SciOpen

Food Science and Human Wellness

journal homepage: https://www.sciopen.com/journal/2097-0765

China Food Publishing Co.

Protective effects of vine tea on high-fat diet rat: regulation of ferroptosis pathway and gut microbiota

Zhu Tao[a,b,c], Junye Li[a], Pinrong Qian[a], Guodong Wu[a], Kexin Hu[a], Yihan Wen[a], Xie He[a], Chunhua Fu[a,c,*], Longjiang Yu[a,c,*]

[a] *Institute of Resource Biology and Biotechnology, Department of Biotechnology, College of Life Science and Technology, Huazhong University of Science and Technology, Wuhan 430074, China*
[b] *Hubei Key Laboratory of Quality Control of Characteristic Fruits and Vegetables, College of Life Science and Technology, Hubei Engineering University, Xiaogan 432000, China*
[c] *Hubei Engineering Research Centre for Dual-use Resource Development of Food and Medicine, Wuhan 430074, China*

ARTICLE INFO

Article history:
Received 16 December 2024
Received in revised form14 January 2025
Accepted 25 January 2025

Keywords:
Vine tea
Dihydromyricetin
High-fat diet rat
Ferroptosis
Lactobacillaceae

ABSTRACT

Vine tea is documented in ancient Chinese books as having the function of promoting blood circulation. However, its effects and mechanisms remain unclear. The aim of this study was to comprehensively investigate the protective potential and mechanisms of vine tea in high-fat diet rat through a combination of *in vivo* and *in vitro* experiments. The efficacy of vine tea was evaluated using a high-fat diet rat model and an oxidized low-density lipoprotein-treated cell model, with physiological and biochemical indicators measured in rat serum and cell supernatants. Transcriptomics was utilized to investigate alterations mRNA expression following the administration of dihydromyricetin in cell model. Metabolomics and 16S rRNA sequencing was employed to examine changes in metabolites in the serum and changes in gut microbiota of high-fat diet rats after administering vine tea extract. Vine tea extract and dihydromyricetin can reduce elevated levels of lipids, including total cholesterol and triglycerides, following modeling. Transcriptomic data indicate that dihydromyricetin exerts its effects by regulating ferroptosis signaling pathways. Metabolomic analysis demonstrates that the administration of vine tea extract influences the vitamin K cycle and glutathione, thereby alleviating the progression of ferroptosis. Additionally, 16S rRNA sequencing reveals that vine tea extract increases Lactobacillaceae in the gut microbiota, which subsequently affects the levels of lysophosphatidylcholine, a major phospholipid component of oxidized low-density lipoprotein in serum. Our results indicate that vine tea can regulate ferroptosis signaling pathways and increase Lactobacillaceae in the gut microbiota, thereby exhibiting cardiovascular protective effects in high-fat diet rats.

1. Introduction

A long-term high-fat diet can lead to abnormal blood lipid levels, promoting the formation of atherosclerosis (AS). AS is a chronic inflammatory disease affecting large and medium-sized arteries. It is characterized by the accumulation of lipids and other blood components in the arterial intima, the proliferation of smooth muscle cells and collagen fibers, and the formation of atheromatous lipid-containing necrotic foci, ultimately leading to sclerosis of the vessel wall[1]. The progression of AS can lead to ischaemic heart disease, ischaemic stroke, and peripheral vascular disease. As a disease of slow progression, clinically significant AS predominantly affects older individuals, despite a decreasing incidence in some countries, continues to be the primary cause of mortality globally[2].

The formation of AS is quite complex and not fully understood at present. The more widely accepted theory suggests that cholesterol, lipids, and cellular metabolic wastes in the blood accumulate in damaged areas of the inner walls of blood vessels, leading to oxidation of cholesterol and subsequent inflammation. Endothelial cells at the damaged sites release active substances that signal monocytes in the blood to migrate towards the damaged area[3]. Stimulated

* Corresponding authors at: College of Life Science and Technology, Huazhong University of Science and Technology, Wuhan 430074, China.
E-mail address: fuchunhua@mail.hust.edu.cn (C.H. Fu); yulongjiang@hust.edu.cn (L.J. Yu)
Peer review under responsibility of Beijing Academy of Food Sciences.

SciOpen Publishing services by Tsinghua University Press

http://doi.org/10.26599/FSHW.2025.9250533

by oxidized cholesterol such as oxidized low-density lipoprotein (ox-LDL), monocytes transform into macrophages, which ingest and digest the oxidized cholesterol molecules, eventually transforming into foam cells that accumulate to form plaques[4]. As these plaques continue to deposit, the arterial wall thickens and hardens, resulting in AS. Currently, the main therapeutic drugs for AS primarily involve 3-hydroxy-3-methylglutaryl coenzyme A reductase inhibitors, such as lovastatin, which can inhibit cholesterol synthesis. However, myotoxic side effects, sometimes severe, including myopathy or rhabdomyolysis, are associated with the use of statins[5]. Ancient Chinese books document numerous plant resources demonstrating therapeutic efficacy in treating cardiovascular and circulatory diseases. Therefore, the bioactive components extracted from herbal sources may serve as a complementary therapy for AS.

Vine tea is a novel food resource made from the tender leaves of the plant *Ampelopsis grossedentata* (Hand.-Mazz.) W. T. Wang, and is generally believed to have the effects of clearing heat, promoting diuresis, calming the liver, lowering blood pressure, and promoting blood circulation. Indeed, some studies suggest that active ingredients in vine tea have the potential to treat cardiovascular-related diseases. Dihydromyricetin (DMY) in vine tea has been shown to protect human umbilical vein endothelial cells through the ERK and Akt-mediated Nrf2/HO-1 signaling pathway[6]. Studies have shown that DMY protects against sodium nitroprusside-induced damage to human vein endothelial cells by activating the PI3K/Akt/FoxO3a signaling pathway[7]. DMY attenuates TNF-α-induced endothelial dysfunction through miR-21-mediated DDAH1/ADMA/NO signal pathway[8]. However, these studies have not explored the mechanisms by which vine tea protects the cardiovascular system in animals on a high-fat diet.

In the present study, we utilized animal and cell experimental models to validate the potential of the active ingredients in vine tea. In an ox-LDL-treated cell model, transcriptomics was employed to investigate the underlying mechanisms of vine tea. Furthermore, a high-fat diet rat model was established to monitor changes in serum metabolites and gut microbiota, thereby providing a multidimensional understanding of vine tea's cardiovascular protective mechanisms.

2. Materials and methods

2.1 Reagents and materials

DMY (CAS# 27200-12-0, purity ≥ 98%) and ox-LDL (catalog number: S24879) were purchased from Yuanye Biotechnology Co., (Shanghai, China).

The water extract of vine tea was prepared as follows. Vine tea was obtained from Zhangjiajie Shenzhoujie Agricultural Industry Development Co., Ltd. (Zhangjiajie, China). Initially, 100 g of vine underwent extraction with 2 L of double-distilled water using sonication for 90 min at a temperature of 80 °C. This extraction process was repeated twice. Subsequently, the resulting solution was collected and dried using a rotary evaporator. Following freeze-drying, a 58 g water extract of vine tea was obtained for use in animal experiments. The water extract was dissolved to saturation in hot water at 80 °C and then cooled to 4 °C for recrystallization. This process was repeated twice to collect recrystallized crystals for use in cell experiments. DMY in the extract was detected using HPLC, with the content of DMY in the aqueous extract measuring 40.70%. After two recrystallizations, the content increased to 93.49%. The residual liquid remaining after these processes should be combined, dried, and utilized for cellular experiments.

The enzyme-linked immunosorbent assay (ELISA) kits used for the analysis of inflammatory factors IL-6 (catalog number: GER0001) and TNF-α (catalog number: GER0004) in AS rats were purchased from Servicebio Biotechnology Co., Ltd. (Wuhan, China). Additionally, the catalase (CAT) assay kit (catalog number: G4307, Servicebio Biotechnology Co., Ltd.) was also utilized. Total glutathione (T-GSH), oxidized glutathione (GSSG) and reduced glutathione (GSH), were measured by T-GSH/GSSG detection kit (catalog number: G4304, Servicebio Biotechnology Co., Ltd.). Various physiological and biochemical indicators in rat serum, including alanine aminotransferase (ALT), aspartate aminotransferase (AST), low-density lipoprotein cholesterol (LDL-C), high-density lipoprotein cholesterol (HDL-C), total cholesterol (TCHO), triglycerides (TG), glutathione reductase (GR), lactate dehydrogenase (LDH), were measured using reagent kits compatible with the Beckman-Coulter AU5800 biochemical analyzer.

The reagents used for the Western blotting (WB) assay, including radioimmunoprecipitation assay (RIPA) buffer, colorimetric bicinchoninic acid (BCA) protein assay kit, and 5× sodium dodecyl sulfate-polyacrylamide gel electrophoresis (SDS-PAGE) protein sampling buffer, were purchased from Servicebio Biotechnology Co., Ltd. (Wuhan, China). Primary antibodies such as NQO1 rabbit pAb (catalog number: A1518), GCLM rabbit pAb (catalog number: A5314), *β*-tubulin rabbit pAb (catalog number: AC008), ColorMixed protein marker 180 (10–180 kDa, catalog number: RM19001) were purchased from ABclonal Technology Co., Ltd. (Wuhan, China). Secondary antibody (DyLight 800, goat anti-rabbit IgG, catalog number: A23920) was purchased from Abbkine Technology Co., Ltd. (Wuhan, China).

2.2 Animals

Several female Sprague-Dawley (SD) rats weighing (200 ± 20) g were obtained from the Hubei Provincial Laboratory Animal Center in Wuhan, China. The rats were accompanied by an Animal Certificate of Conformity of SCXK (E) 2020-0018, certifying their origin and compliance with animal welfare regulations. The animal care and handling protocols were reviewed and approved by the Animal Ethics Committee of the College of Life Science and Technology, Huazhong University of Science and Technology.

2.3 Cell culture and experimental modeling

The cellular experimental models of high-fat diet were mainly created by treating cells with 50 μg/mL ox-LDL[9-11]. RAW264.7 cells, a mouse macrophage cell line, were was obtained from the Cell Bank of the Chinese Academy of Sciences (Shanghai, China). The RAW264.7 cells were cultured under standard conditions, involving incubation at 37 °C in a 5% CO_2 atmosphere. The culture medium used for the cells was Dulbecco's modified Eagle's medium (DMEM) supplemented with penicillin (100 U/mL), streptomycin (100 μg/mL), and 10% fetal bovine serum (Gibco, USA). These components provided the necessary nutrients and growth factors for cell growth and maintenance.

For each experiment, cells in the exponential growth phase were utilized. The cells were cultured in serum-free medium for 24 h before drug treatment. The experimental cell groups were structured as follows: the control group received no drug treatment, the model group was exposed to ox-LDL at a concentration of 50 μg/mL. The treatment groups were subjected to the same concentration of ox-LDL, with DMY added at concentrations of 25, 50, 100, and 200 μg/mL, respectively, 2-h prior to the ox-LDL treatment.

To investigate the therapeutic effects of components in vine tea extract after removing DYM, the treatment groups were also exposed to the same concentration of ox-LDL, with one group receiving 200 μg/mL of DMY and another receiving 200 μg/mL of extract with DMY removed after crystallization. After 24 h, the cell culture supernatant was collected, and the concentrations of TG and TCHO in the supernatant were measured.

2.4 Administration of vine tea extracts and drugs to the high-fat diet rat

The high-fat diet feed (catalog number: XT109C) was purchased from Xietong Medical Bioengineering Co., Ltd. (Nanjing, China), and it complies with the regulations of GB 13078–2017 and GB/T 14924.2–2001. To establish an AS rat model, a combination of a high-fat diet and vitamin D_3 (VD_3) injections was employed[9]. After one week of adaptation feeding, the rats began modeling, and the entire modeling process lasted for 12 weeks. VD_3 (600 000 IU/kg) was injected intraperitoneally before modeling, and 100 000 IU/kg was injected at 2, 4, 6, 8, and 10 weeks after modeling. Additionally, the rats were fed a high-fat diet throughout the modeling process to induce the AS model. SD rat were randomly assigned to six groups, each consisting of eight rats. The groups included Control group (NC), AS model group (M), and oral gavage administration during modeling groups. The gavage treatment group included the following subgroups: gavage administration of simvastatin group (PC, 5 mg/kg), low-dose water extract of vine tea group (LWE, 50 mg/kg), middle-dose water extract of vine tea group (MWE, 100 mg/kg), high-dose water extract of vine tea group (HWE, 250 mg/kg).

2.5 Determination of biochemical indicators and histopathological observations

After 12 weeks of modeling, rat feces were collected and stored in a –80 °C freezer for gut microbiota analysis. Subsequently, the rats were anesthetized, and blood was collected into blood collection tubes. After clotting, the tubes were centrifuged at 2 000 r/min for 15 min at 4 °C. The resulting supernatant was collected, aliquoted, and stored at –80 °C. Some serum samples were used for non-targeted metabolomics analysis, while others were used to measure biochemical indicators such as ALT, AST, LDL-C, HDL-C, TCHO, TG, GR, LDH, CAT, IL-6 and TNF-α.

After blood collection, the rats were euthanized. The aorta was isolated, washed twice with PBS, and then cut into sections. Some sections were fixed in tissue fixative for hematoxylin and eosin (HE) staining, while another portion was frozen at –80 °C for oil red O staining.

Additionally, rat liver samples were collected and analyzed alongside serum samples for indicators associated with ferroptosis, including GSH, T-GSH and GSSG.

2.6 Transcriptomic analysis

Transcriptome samples of cells were categorized into three groups: the blank control group, model group, and treatment group, each containing three parallel samples. The blank control group did not undergo any drug treatment, while the model group was exposed to 50 μg/mL ox-LDL. In the treatment group, cells were pre-treated with 200 μg/mL DMY for 2 h before being exposed to 50 μg/mL ox-LDL. The cells were washed twice with PBS at 4 °C, vigorously lysed with TRIzol reagent in each culture dish, and the resulting TRIzol solution was collected. After rapid freezing in liquid nitrogen for 2 h, the samples were stored at –80 °C before being sent to a transcriptome sequencing company for analysis.

After completing the cellular experiments, a total of nine samples from three groups of cells were sent to Majorbio Technology Co., Ltd. (Shanghai, China) for testing. The samples were divided into three groups as follows: blank group (group A): samples A1, A2, A3; ox-LDL-treated model group (group B): samples B1, B2, B3; DMY drug group (group C): samples C1, C2, C3. Each group comprised three samples. These samples underwent sequencing using the Meiji Medical Reference Transcriptome Sequencing Platform to conduct comprehensive transcriptome analysis on all nine samples. The raw reads were deposited into the NCBI Sequence Read Archive (SRA) database (BioProject accession: No. PRJNA1135337).

2.7 Metabolomics analysis

Serum samples were obtained after AS animal model modelling was performed. A total of 18 serum samples from three groups of rats were submitted to MetWare Technology Co., Ltd. (Wuhan, China) for non-targeted metabolomics testing. The samples were categorized into three groups as follows: blank group (group A): samples A1 to A6; AS rat model group (group B): samples B1 to B6; high-dose water extract of vine tea group (group C): samples C1 to C6. Each group consisted of six samples, with the samples labeled consistently as the serum samples originated from the same rats. The test data was analyzed, processed, and visualized using the MetWare Cloud, a free online platform for data analysis (https://cloud.metware.cn).

2.8 Gut microbiota analysis

On the day preceding the conclusion of the AS rat experiment, fecal samples were collected. A total of 18 feces samples from three groups of rats were submitted to MetWare Technology Co., Ltd. (Wuhan, China) for 16S rRNA sequencing testing. The samples were categorized into three groups in accordance with the non-targeted metabolomics testing protocol, as they were derived from the same rats.

2.9 Gene analysis by PCR

The cells used for PCR have the same cell modelling steps described in section 2.3. After 24 h, the cells were washed twice with PBS at 4 °C, vigorously lysed with TRIzol reagent, and the resulting TRIzol solution was collected. The primers utilized for amplifying *Nqo1* and *Gclm* expression were as follows: *Nqo1* forward: 5′-TATCCTTCCGAGTCATCTCTAGCA-3′, reverse: 5′-TCTGCAGCTTCCAGCAGCTTCTTG-3′.

Gclm forward: 5′-GAAGACATCATTCAACTACGCC-3′, reverse: 5′-GAGATGACTCGGAAGGATACT-3′. The reference gene *GAPDH* was employed for normalization. The target mRNA levels were normalized against *GAPDH* mRNA, and the gene expression relative to the control group was determined using the $2^{-\Delta\Delta Ct}$ method. The relative mRNA expression was presented as fold expression over the average expression of the control group.

2.10 WB analysis

After 24 h, the cells were washed twice with PBS and lysed on ice using RIPA buffer for WB analysis. The protein concentration in the lysate was determined using a colorimetric BCA protein assay kit. Subsequently, the protein samples were separated by 10% SDS-PAGE and transferred onto PVDF membranes. Following this, the PVDF membranes were blocked with a blocking solution for 2 h at room temperature. Primary antibodies were then incubated with the PVDF membranes overnight at 4 °C. The membranes were washed three times with TBST (Tris-buffered saline with Tween 20) for 5 min each. Next, secondary antibodies were added and incubated at 37 °C for 2 h. Finally, protein bands were detected using a dual-color infrared laser system (Odyssey_CLx, LI-COR Inc., USA).

2.11 Statistical analysis

The statistical analysis was conducted using SPSS 17.0 software. The data was graphed using Origin and Prism software. The data were presented as mean ± standard deviation (SD). To evaluate the differences between multiple groups, a one-way analysis of variance (ANOVA) was performed. A significance level of $P < 0.05$ was considered statistically significant.

3. Results

3.1 DMY decreases elevated levels of TG and TCHO induced by ox-LDL in RAW264.7 cells

The impact of DMY on TG and TCHO was investigated in cells treated with ox-LDL. DMY had a significant effect on TCHO at 50 μg/mL, but the effect on TG was not significant until 200 μg/mL (Figs. 1A and B). Consequently, when designing the experiment for transcriptome analysis, we selected a DMY concentration of 200 μg/mL. In addition, after removing DMY through recrystallization, it can be observed that the remaining vine tea components have no significant regulatory effect on TG and TCHO (Figs. 1C and D). This result indicates that DMY is the primary component in the water extract of vine tea that is responsible for its effect on reducing TG and TCHO levels.

3.2 Cell transcriptome analysis indicates that DMY can inhibit lipid metabolism disorders by regulating the ferroptosis pathway

We employed transcriptomics to investigate the mechanism by which DMY reduces elevated levels of TG and TCHO induced by ox-LDL in RAW264.7 cells. The transcriptome analysis of nine samples has been completed, yielding a total of 57.82 Gb of clean data, with each sample generating more than 6.06 Gb of clean data and a Q30 bases percentage exceeding 95.95%. Genome comparison and localization were conducted for all samples using the following reference information: Reference gene source: *Mus_musculus*; Reference genome version: GRCm39; Reference genome source: https://mart.ensembl.org/Mus_musculus/Info/Index. Statistical analysis was performed to compare gene expression between different subgroups. Among these, 10 841 genes were expressed in all three groups, 291 genes were expressed exclusively in the blank group, 149 genes were expressed exclusively in the model group, and 253 genes were expressed exclusively after drug administration (Fig. 2A). Based on the quantitative expression results, differential gene analysis was performed on the Meggie Bio platform. DESeq2 was used as the software for the differential analysis, with screening thresholds set at $|\log_2 FC| \geq 0.07$ and adjusted P-value (P_{adj}) < 0.05. The model group demonstrated significant down-regulation of 893 genes and significant up-regulation of 698 genes compared to the blank group, further corroborating the success of cell modeling. In contrast, the administered group exhibited significant down-regulation of eight genes and significant up-regulation of three genes compared to the model group (Fig. 2B).

To investigate the changes in cellular gene regulation following ox-LDL treatment of macrophages and to provide a reference for further studies of this cell model, we performed functional annotation and enrichment analysis on the target genes identified from the differential genome. The experimental results indicated that there were more changes in genes related to the circulatory, endocrine, and immune systems after ox-LDL treatment of cells. Notably, the significant changes in metabolism-related genes were primarily associated with lipid metabolism (Fig. 2C).

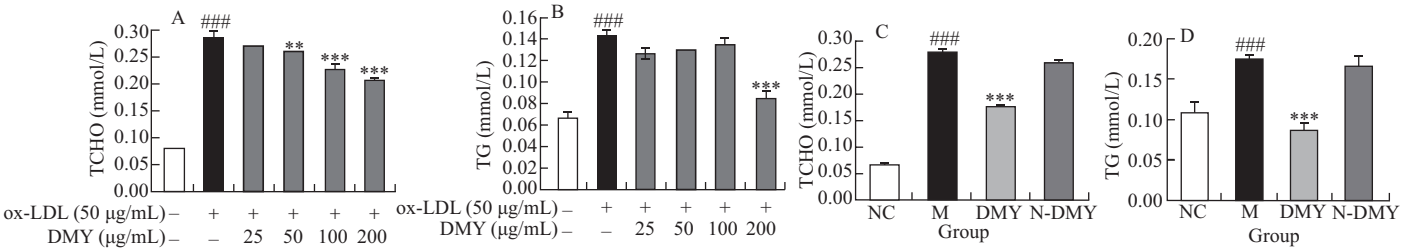

Fig. 1 DMY reduces lipid levels in cell supernatants in RAW264.7 cells treated with ox-LDL. (A, B) Changes in TCHO and TG levels in cell supernatants after modeling and administration of different concentrations of DMY. (C, D) Changes in TCHO and TG levels in the supernatants of cells after modeling and administration of 200 μg/mL DMY or extract with DMY removed after crystallization (N-DMY).
$^{###}P < 0.001$ *vs.* the control group; $^{**}P < 0.01$, $^{***}P < 0.001$ *vs.* model group.

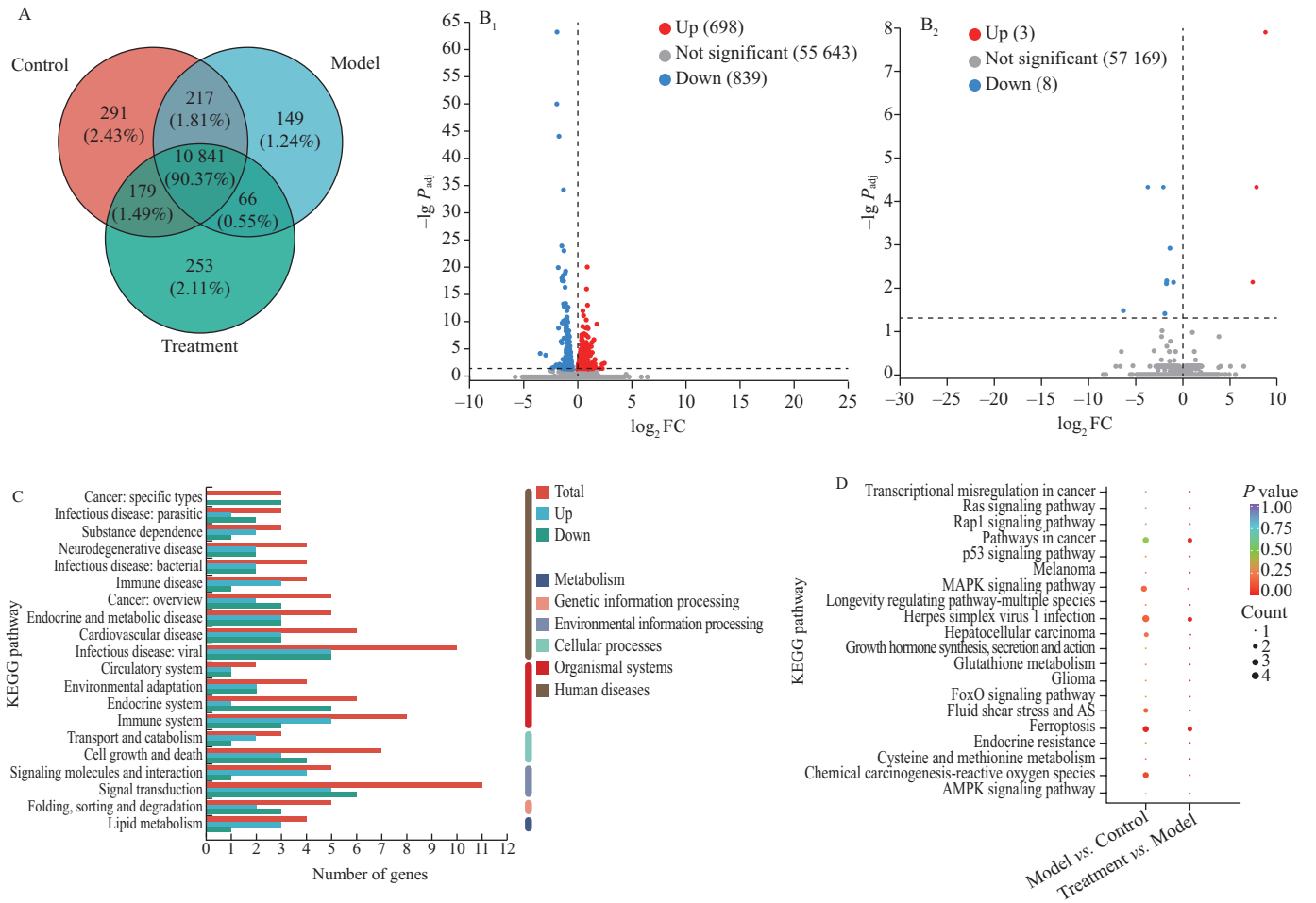

Fig. 2 Transcriptomics analysis was conducted among different groups following ox-LDL modeling (model group), 200 μg/mL DMY administration (treatment group), and the control group. (A) Venn diagram illustrates the overlap of gene expression between samples from different subgroups. Volcano plots for the differential genes between (B_1) control *vs*. model group and (B_2) model group *vs*. treatment group. (C) Functional annotation analysis plot of differential genes in the model group *vs*. control group. (D) Enrichment analysis of differential genes in KEGG signaling pathways was conducted following the comparisons of control group *vs*. model group and model group *vs*. treatment group, resulting in a shared KEGG signaling pathway diagram.

To identify the pathways through which DMY exerts its therapeutic effects, we combined the signaling pathways of the control *vs.* model and model *vs.* drug groups to identify the shared KEGG signaling pathways. The results showed that genes related to ferroptosis and fluid shear stress and AS were significantly altered after modeling and drug administration (Fig. 2D). This suggests that DMY may exert its effects through these signaling pathways. The genes corresponding to these pathways include *Nqo1* and *Gclm*.

Ferroptosis is a form of cell death characterized by the excessive accumulation of lipid peroxides resulting from disruptions in intracellular metabolic pathways. Transcriptomic was empolyed to analyze relevant pathways in cells treated with ox-LDL and DMY. We found that modeling with ox-LDL resulted in changes to genes associated with lipid metabolism. This finding aligns with our observation of increased TG and TCHO levels in the cell supernatant following treatment. After DMY administration, alterations were observed in ferroptosis-related pathways, with significant changes noted in the genes *Nqo1* and *Gclm*. These results demonstrate that DMY can regulate ferroptosis-related pathways, thereby mitigating lipid dysregulation.

3.3 Water extract of vine tea reduces blood lipids and prevents vascular lesions in high-fat diet-induced AS rats

The study investigated the therapeutic effects of vine tea using a high-fat diet-induced AS rat model. Specifically, water extract of vine tea was orally administered to rats that were exposed to a high-fat diet and VD_3 injections, which is known to induce AS.

The results demonstrated significant decreases in lipid indicators (TCHO, TG, and LDL-C), liver function indicators (ALT, AST), inflammatory factor indicators (IL-6, TNF-α), and oxidative stress indicators (LDH, CAT, and GR) after administering water extract of vine tea (Fig. 3). It is noteworthy that following the modeling, there was no significant change in the HDL-C index. However, the TG index was significantly reduced only after administering medium and high doses of water extract from vine tea. Overall, significant changes were observed in most physiological and biochemical indicators in the serum of AS model rats following administration of vine tea extract. These findings suggest that the water extract of vine tea may have a therapeutic effect on AS.

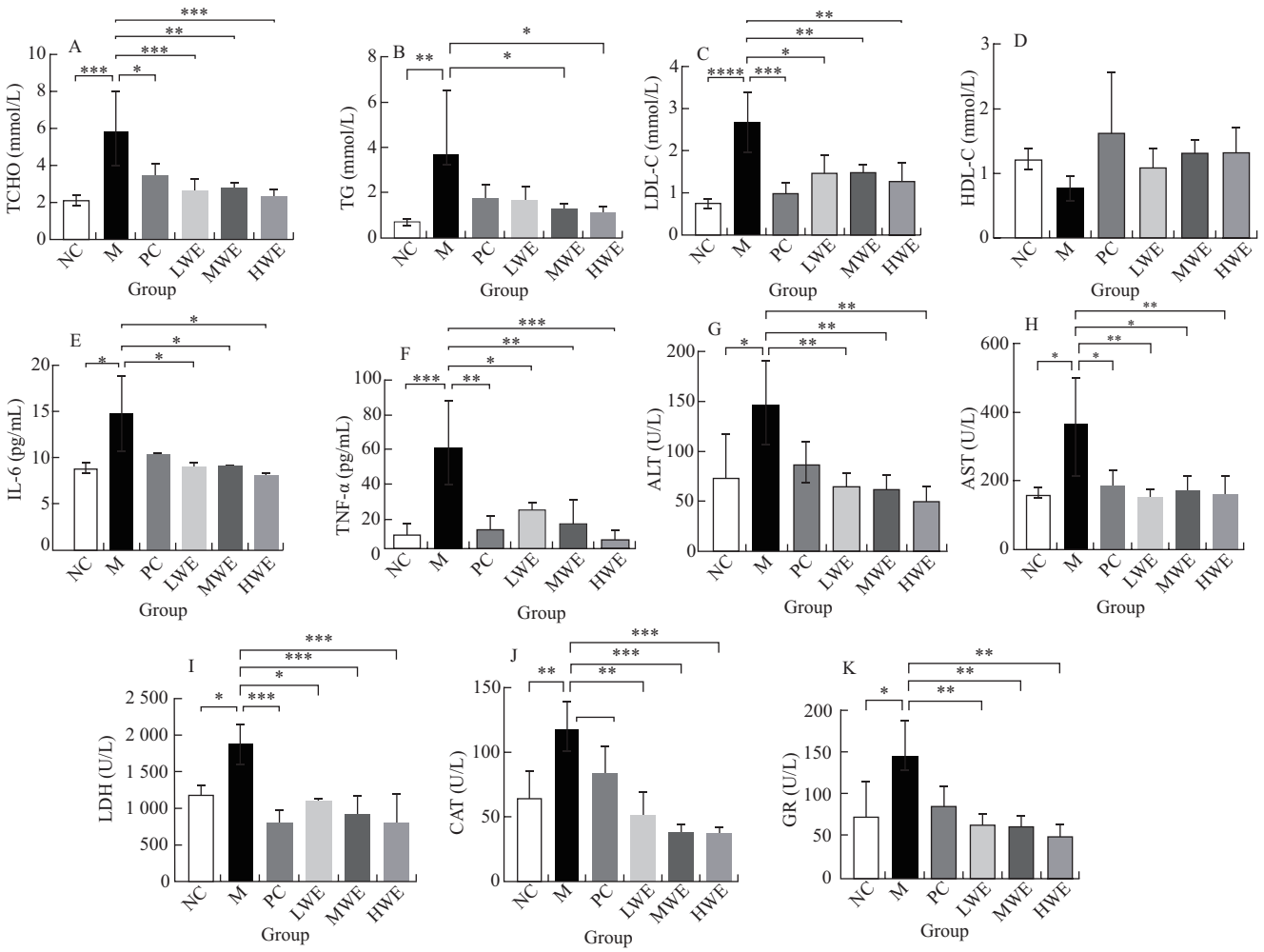

Fig. 3 The therapeutic effects of vine tea in an AS animal model induced by a high-fat diet and VD_3 injections. (A) TCHO, (B) TG, (C) LDL-C, (D) HDL-C, (E) IL-6, (F) TNF-α, (G) ALT, (H) AST, (I) LDH, (J) CAT, and (K) GR level in serum. *$P < 0.05$, **$P < 0.01$, ***$P < 0.001$, and ****$P < 0.000\ 1$.

Detection was studied by HE staining and oil red O staining of the blood of the different groups (Fig. 4). The HE-stained sections were observed at 100× magnification, and the oil red O-stained sections were magnified 400-fold for analysis. HE-stained images illustrate that the vessel walls in the control group exhibited uniform thickness and smoothness. In contrast, the AS model group displayed uneven vessel wall thickness and the presence of breaks. When vine tea extract was administered during the modeling, the LWE group still showed vessel wall breakage, whereas a higher dose resulted in uniform vessel wall thickness without breakage in the HWE group. The oil red stained picture shows the same outcome where red areas indicate lipid deposits. The arterial vessel walls of the control group did not exhibit any lipid deposition. In contrast, the model group rats' arterial vessels showed significant lipid deposition after modelling, indicating a successful modeling effect. Conversely, after administering the drug, lipid deposition decreased in the LWE group while no lipid deposition was observed in the high-dose extract group. The above results showed that the administration of vine tea water extract demonstrated a positive effect on these pathological changes in the arterial blood vessels.

3.4 Water extract of vine tea prevents AS through modulation of the linoleic acid and glycerophospholipid metabolic pathway

To investigate the impact of the aqueous extract of vine tea on the process of high-fat diet-induced AS, we employed metabolomics to analyze the metabolites in the serum of the control group, the model group, and the high-dose treatment group. Focusing on metabolites with significant changes between groups, 243 metabolites with significantly down-regulated levels and 206 metabolites with significantly up-regulated levels were identified in the serum of the blank group compared to the model group. Additionally, in comparison to the high dose administration group, the model group exhibited 145 metabolites with significantly down-regulated levels and 38 metabolites with significantly up-regulated levels (Fig. 5A). We conducted KEGG pathway enrichment analysis for metabolites that differed between groups and identified that these metabolites were primarily associated with linoleic acid metabolism and glycerophospholipid metabolism (Fig. 5B). The differences in metabolite content related to linoleic acid between groups are illustrated (Fig. 5C), while the differences in metabolite content related to glycerophospholipids between groups are displayed (Fig. 5D). Metabolomics results suggest that vine tea extract may help slow down AS induced by a high-fat diet through modulation of lipid metabolism, including linoleic acid metabolism and glycerophospholipid metabolism.

3.5 *Long-term administration of water extract of vine tea leads to changes in the gut microbiota in high-fat diet-induced AS rats*

To clarify the impact of long-term oral administration of vine tea extract on the intestinal microbiota and its correlation with changes in serum metabolites, we utilized 16S rRNA sequencing to characterize the intestinal flora followed by detailed data analysis. Following modeling, there was a decrease in the relative abundance of Firmicutes in the rat intestinal flora, which subsequently increased after administration of vine tea extract (Fig. 6A). Particularly notable was the increase in Verrucomicrobiota following modeling with a high-fat diet, while decreased after vine tea extract administration. Through LEfSe analysis, it was found that after modeling with a high-fat diet, the increased Verrucomicrobiota

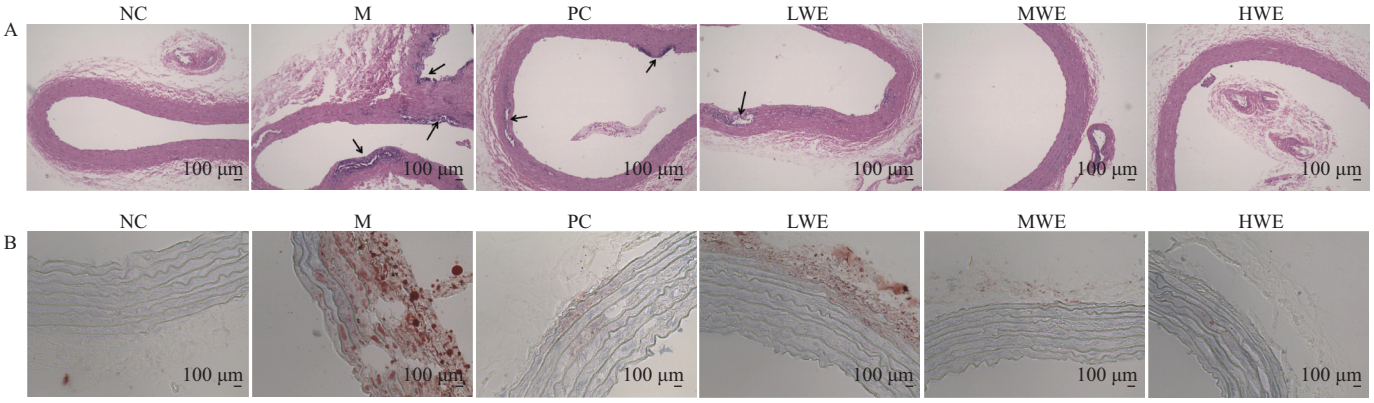

Fig. 4 (A) HE-stained images of arterial blood vessels from AS rats following modeling and drug administration revealed lesions at the sites indicated by arrows, as shown in the 100× magnification images. (B) Oil red O staining demonstrates the presence of lipid accumulation (indicated by reddish coloration) in the arterial vessel wall following modeling, as depicted in the 400× magnification images.

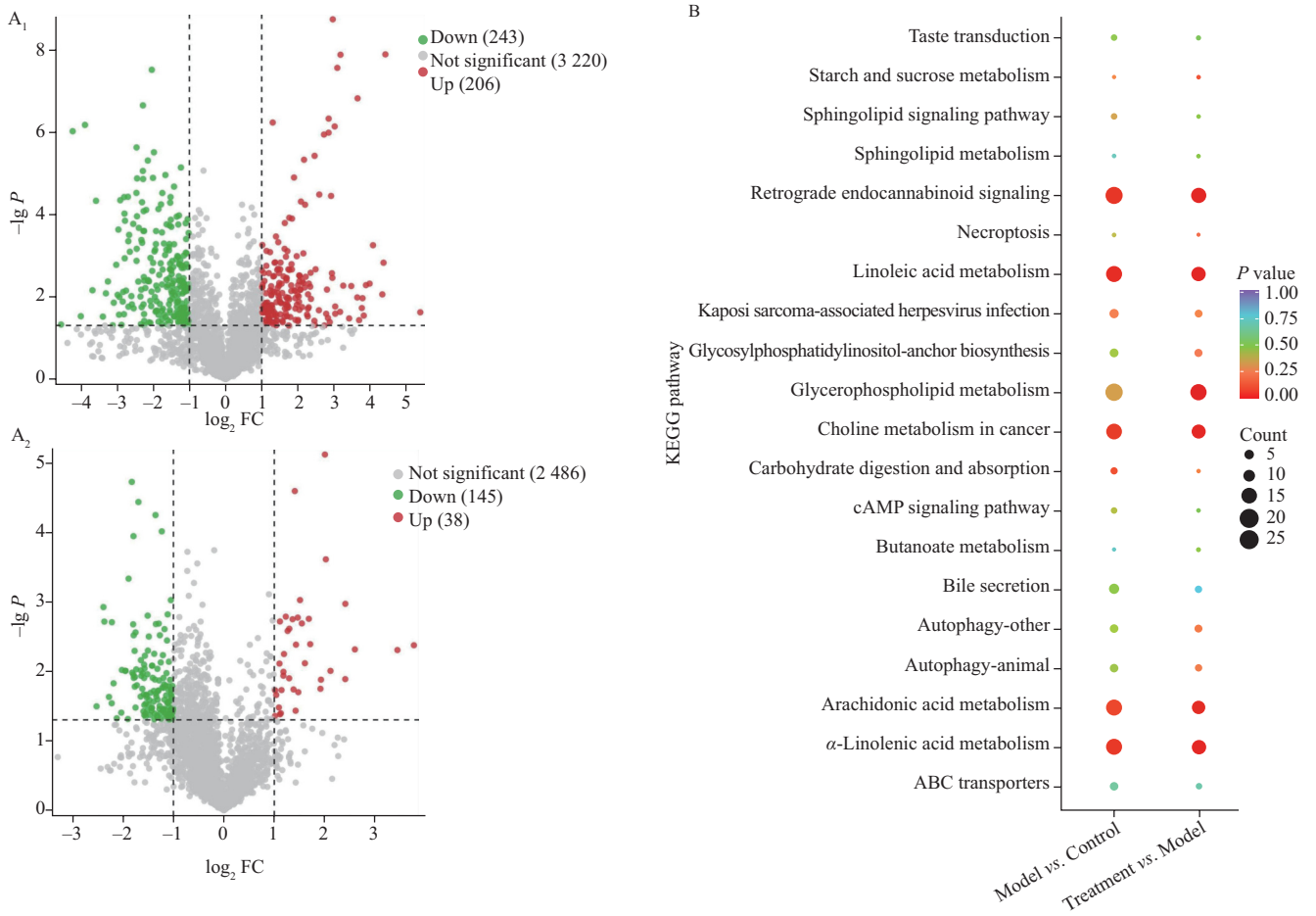

Fig. 5 Metabolomics analysis was conducted between different groups following AS modeling (model group), vine tea extract administration (treatment group), and the control group. (A) Volcano plots for the differential metabolites between (A_1) control group *vs*. model group and (A_2) model group *vs*. treatment group were created. (B) Enrichment analysis of differential metabolites in KEGG signaling pathways was conducted following the comparisons of model group *vs*. control group and treatment group *vs*. model group , resulting in a shared KEGG signaling pathway diagram. Heatmaps of differential metabolites in (C) linoleic acid metabolism-related pathway and (D) glycerophospholipid metabolism-related pathway.

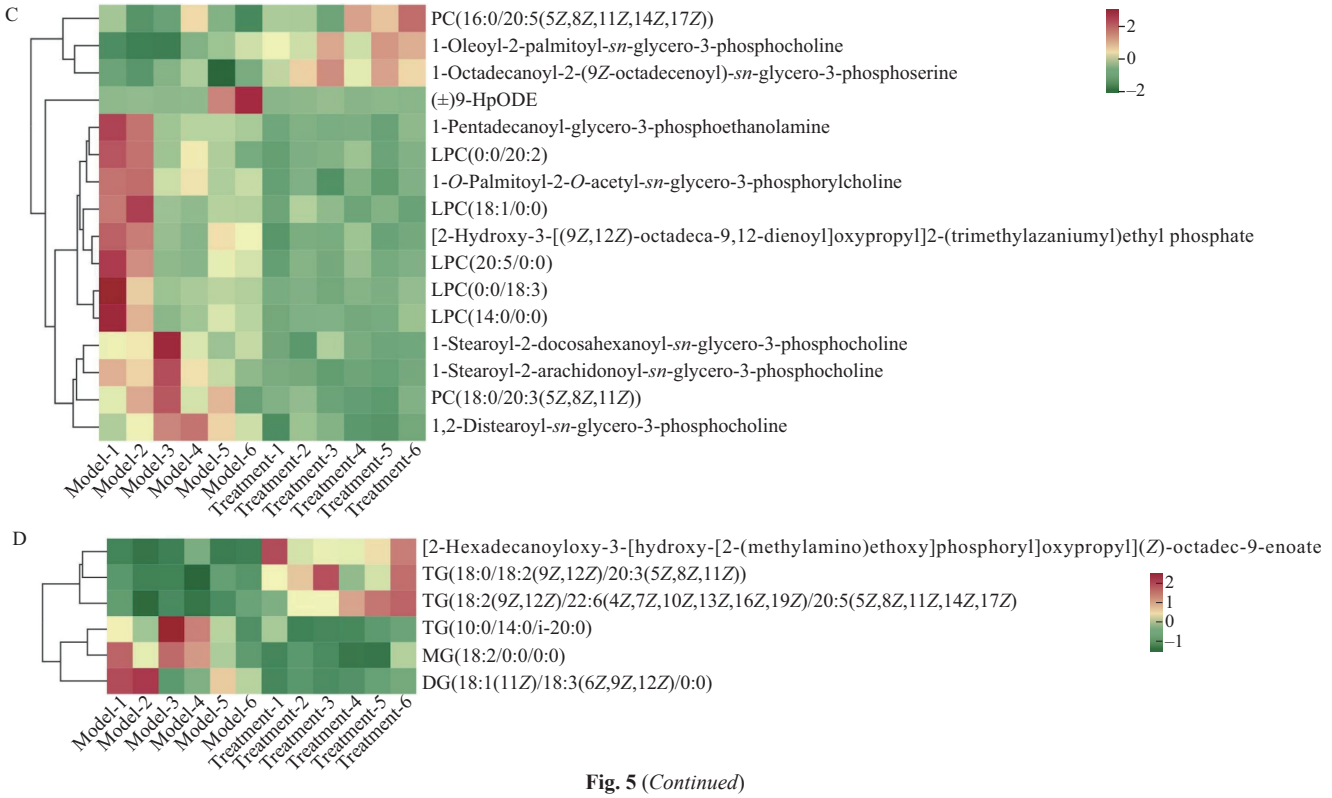

Fig. 5 (*Continued*)

is predominantly represented by Akkermansiaceae, whereas after administration of the vine tee extract, the increased abundance is mainly composed of Lactobacillaceae, specifically lactobacilli, which belong to the Bacilli class (Figs. 6B and C). Using Spearman correlation analysis between metagenomics and differential serum metabolomics, it was found that changes in gut microbiota correlate significantly with certain differentially abundant metabolites in the serum. For instance, metabolites such as LPC(20:2) related to linoleic acid metabolism and TG(10:0/14:0/i-20:0) related to glycerophospholipid metabolism, show significant correlations with Bacilli (Fig. 6D). This demonstrates that long-term high-fat diet and administration of vine tea extract can alter gut microbiota, thereby influencing serum metabolites and affecting the progression of AS.

3.6 DMY can influence the ferroptosis signaling pathway in both cellular and animal models

Afer cellular modeling, we utilized qPCR and WB to analyses to validate the expression and protein levels of the two important genes mentioned above, *Nqo1* and *Gclm*. The results showed that after ox-LDL treatment, the expression of *Nqo1* and *Gclm* genes (Figs. 7A and B), as well as the levels of their related proteins (Figs. 7C and D), decreased in the cells. However, after administration of DMY, the expression of these two genes and their protein levels increased significantly. This indicates that DMY can indeed up-regulate the expression of *Nqo1* and *Gclm*. This result was consistent with the transcriptome data.

In animal models, we analyzed ferroptosis-related metabolites. By exploring the KEGG signaling pathway for ferroptosis, we found that GSH was closely associated with *Gclm*, while vitamin K was closely associated with *Nqo1*. Cell experiments confirmed that DMY can up-regulate the expression of the *Nqo1* gene. In the serum metabolites of the animals, we observed a significant decrease in the content of the related metabolite, vitamin K (Fig. 7E), following the administration of the vine tea water extract. Thus, by integrating metabolomics and transcriptomics data, we conclude that vine tea can upregulate the *Nqo1* gene associated with the ferroptosis pathway, thereby reducing the levels of the downstream metabolite, vitamin K. Cell experiments confirmed that DMY can upregulate the expression of the *Gclm* gene. However, no significant changes were observed in the levels of another serum metabolite, GSH (Fig. 7F). This is because the relative content of GSH in the metabolomics data represents T-GSH and does not differentiate between GSSG and GSH. Therefore, we remeasured the levels of T-GSH, GSSG, and GSH in serum and liver tissues (Figs. 7G and H). The results were consistent with our expectations, demonstrating a significant increase in GSH levels, which were positively correlated with the expression of *Gclm*. Our experimental results indicate that, in both cellular and animal models, DMY can influence the ferroptosis signaling pathway.

4. Discussions

In this study, we employed ox-LDL-treated RAW264.7 cells to explore the mechanism of DMY, which is the principal active compound in vine tea water extract. Transcriptomic was utilized to investigate the mechanism of DMY action. Additionally, we evaluated the therapeutic effects of aqueous extract from vine tea in a rat model of AS, which was induced by a high-fat diet and VD_3 injection. Metabolomic and 16S rRNA analyses were performed to examine the mechanisms of vine tea extract. Our research contributes to the understanding of a novel mechanism through which DMY may exert its effects on on high-fat diet animals.

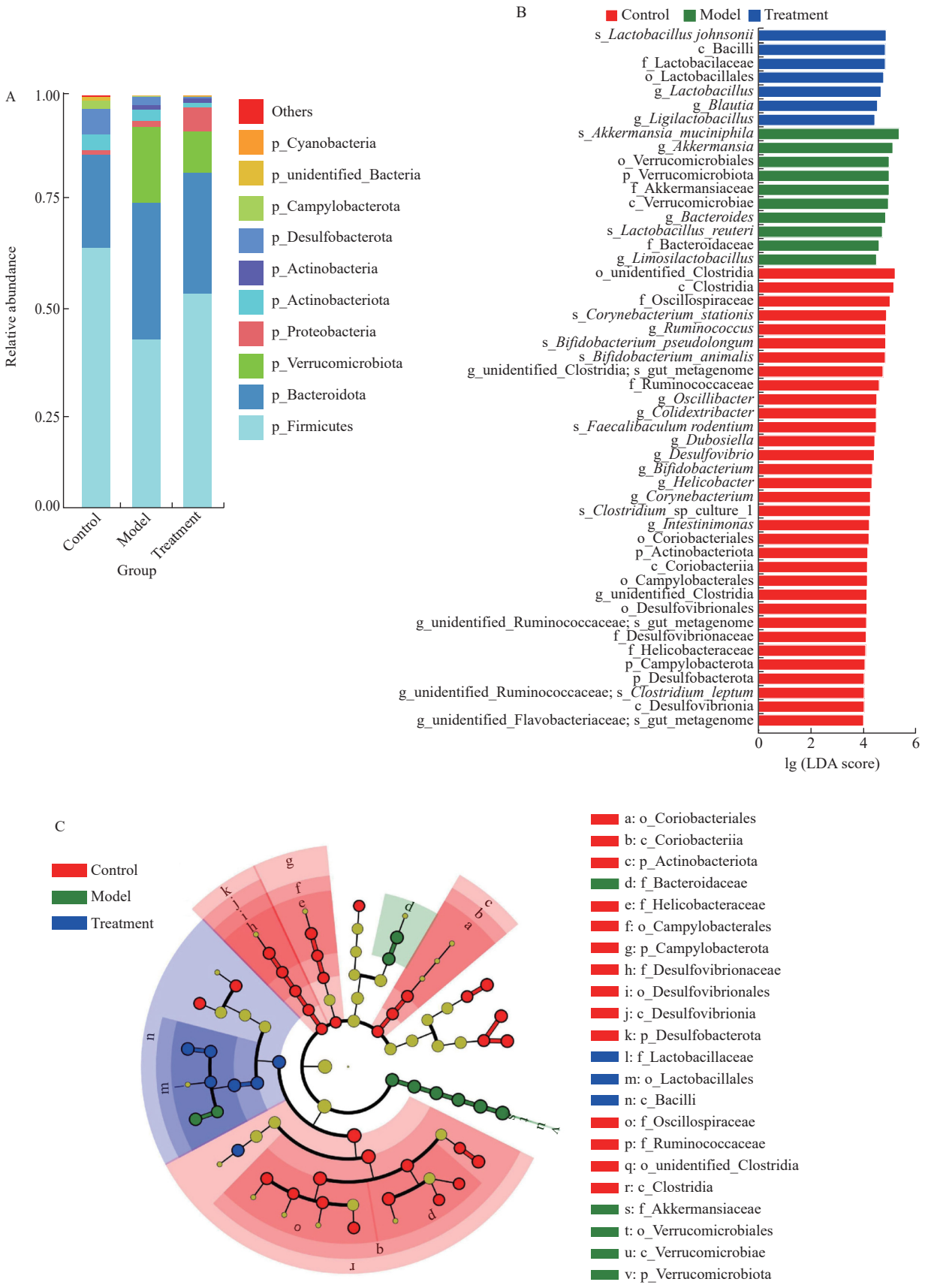

Fig. 6 16S rRNA sequencing analysis results of gut microbiota in different groups. (A) Comparison of gut microbiota abundance at the phylum level across different groups. (B) Bar plot based on the LEfSe analysis among the different groups. (C) Cladogram based on the LEfSe analysis results among the different groups. (D) Spearman correlation analysis results between differential metabolites and differential gut microbiota.

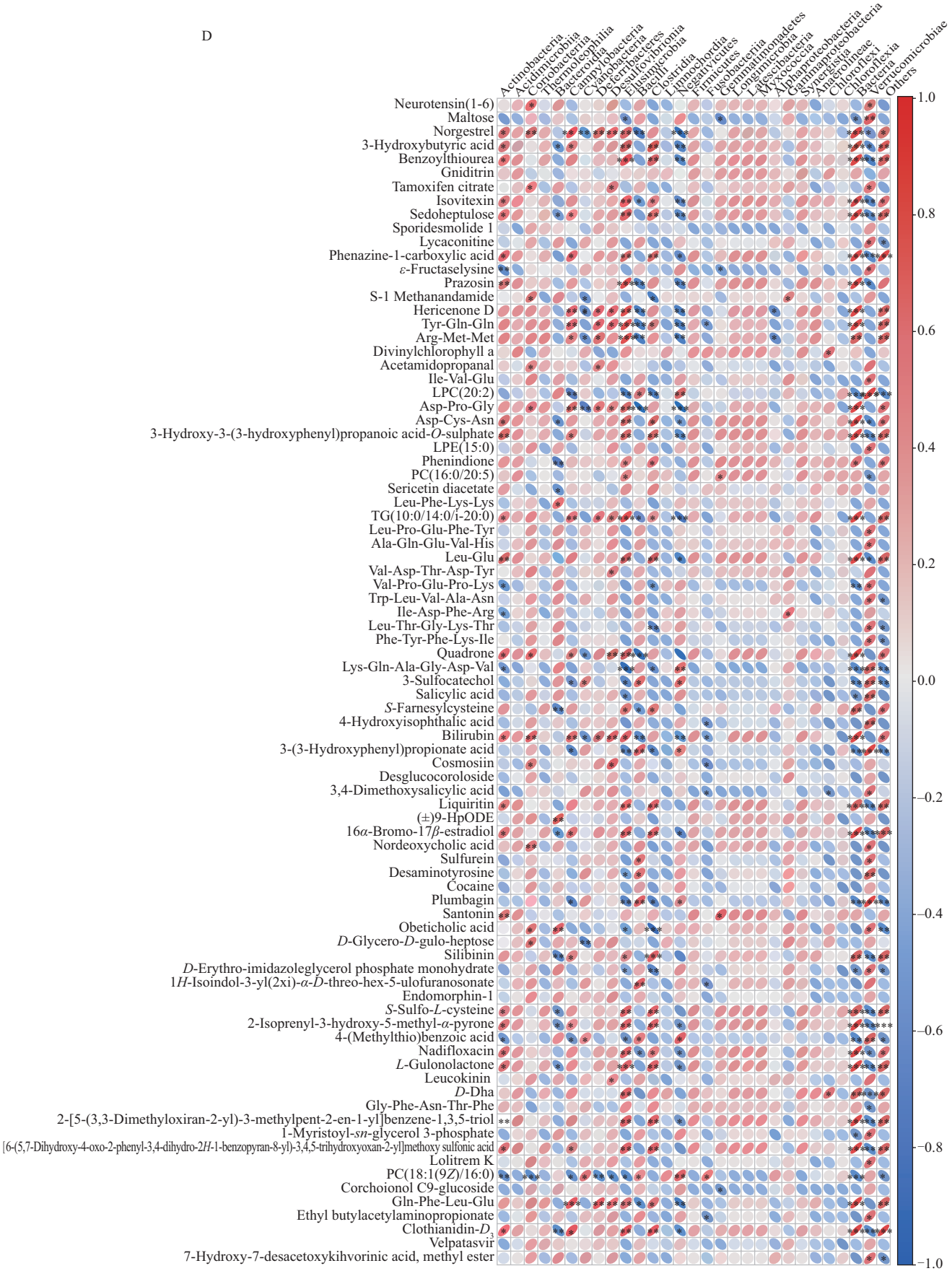

Fig. 6 (*Continued*)

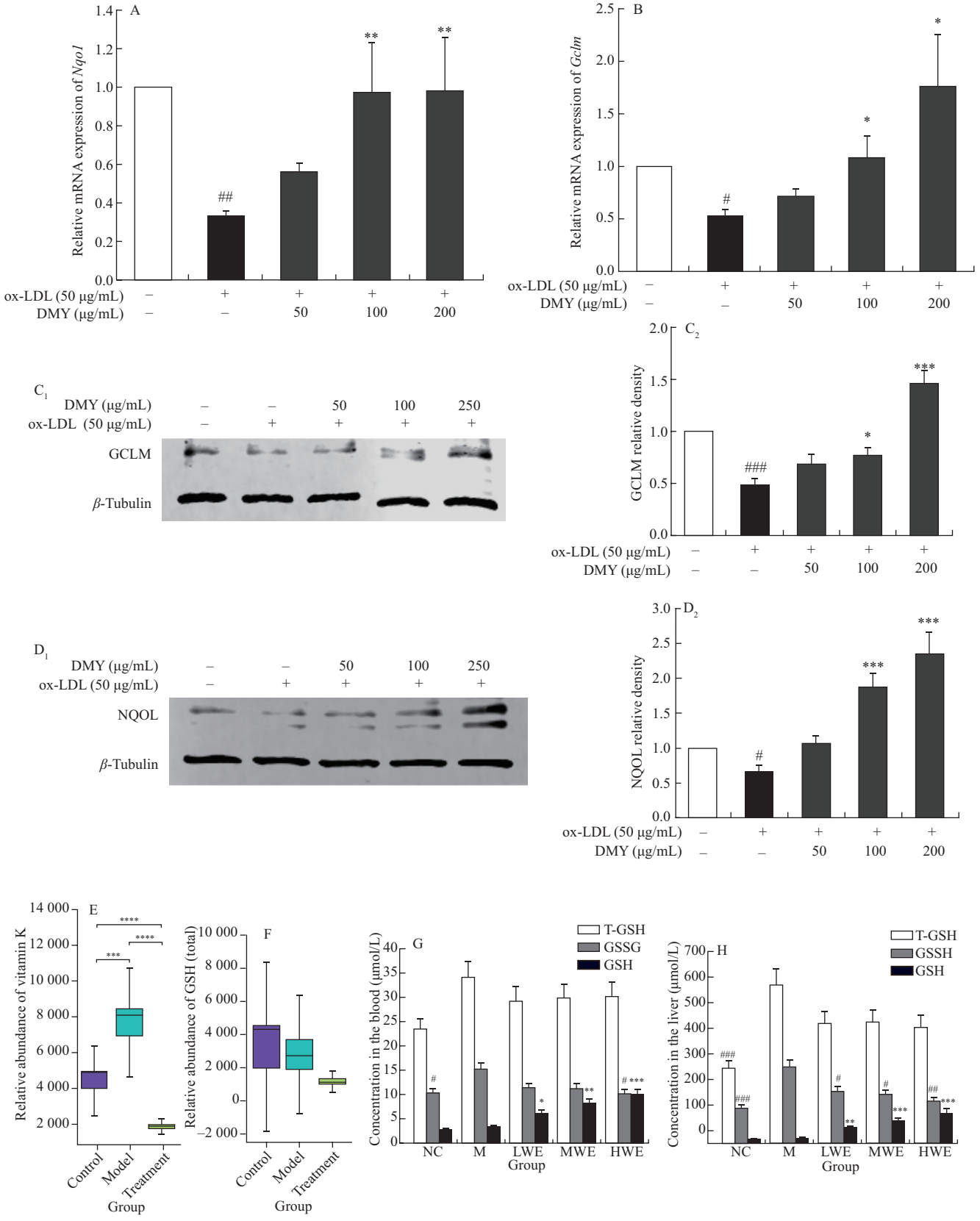

Fig. 7 Changes in genes, proteins, and related compounds associated with the ferroptosis signaling pathway in a cell model and an AS rat model. (A, B) Changes in gene expression of *Nqo1* and *Gclm* after modeling and administration of different concentrations of DMY ($n = 3$). (C, D) Changes in NQO1 and GCLM protein levels after modeling and administration of different concentrations of DMY ($n = 3$). (E, F) The relative content of metabolites related to ferroptosis, vitamin K and glutathione was analyzed across different groups. (G, H) Levels of T-GSH, GSSG, and GSH in serum and liver tissues were measured across different groups. $^{\#}P < 0.05$, $^{\#\#}P < 0.01$, $^{\#\#\#}P < 0.001$ *vs*. control group;$^{*}P < 0.05$, $^{**}P < 0.01$, $^{***}P < 0.001$ *vs*. model group.

The extract of vine tea and its main component DMY have the function of regulating lipid disorders. After treating the cells with ox-LDL to establish a model, we observed lipid dysregulation, evidenced by a significant increase in TG and TCHO levels in the cell supernatant (Fig. 1). Concurrently, transcriptomic data revealed substantial changes in the expression of genes associated with lipid metabolism (Fig. 2C). After administration of DMY, the levels of TG and TCHO in the cell culture supernatant significantly decreased, demonstrating that DMY has a favorable regulatory effect on lipid metabolism (Figs. 1A and B). It is worth noting that, after removing DMY through recrystallization, it can be observed that the remaining vine tea components have no significant regulatory effect on TG and TCHO (Figs. 1C and D). This result indicates that DMY is the primary component in the water extract of vine tea responsible for its effects on regulating lipid disorders.

To clarify the regulating lipid disorders mechanism, transcriptomics was used to study the effects of DMY on gene expression and signaling pathways in cells treated with ox-LDL. The results indicated that genes associated with ferroptosis, fluid shear stress and AS were significantly altered following modeling and drug administration (Fig. 2D). This suggests that DMY may exert its effects through these signaling pathways. Previous studies have shown that DMY suppresses hepatic lipid accumulation and increases the mRNA and protein expressions of ATP-binding cassette transporter A1 (ABCA1), PPARα, LXRα, and ABCA1[10,12]. However, the significant changes in these genes described in the literature have not been observed in our transcriptomics data. Our experimental results suggest that DMY may regulate lipid metabolism by modulating the expression of genes and proteins, such as *Gclm* and *Nqo1*. To further confirm whether DMY can upregulate these two genes, we utilized qPCR and WB analyses to validate the expression and protein levels of the aforementioned important genes. The results indicated that following ox-LDL treatment, the expression levels of the *Nqo1* and *Gclm* genes (Figs. 7A and B), as well as the levels of their corresponding proteins (Figs. 7C and D), decreased in the cells. However, after the administration of DMY, the expression of these two genes and their protein levels increased significantly. These results are highly consistent with the transcriptomic data. We can preliminarily conclude that DMY regulates the ferroptosis pathway, including the *Gclm* and *Nqo1* genes, and further regulates lipid metabolism. In fact, reaching this conclusion is not difficult to understand. Ferroptosis is caused by lipid peroxidation, which is controlled by integrated oxidation and antioxidant systems[13-14]. The drug used to treat cells, ox-LDL, is a lipid peroxide that results from a long-term high-fat diet[15-16]. In addition, literature reports have confirmed that DMY can treat various diseases, such as acute kidney injury[17], cerebral ischemia-reperfusion injury[18], and type 2 diabetic cognitive impairment[19], by affecting ferroptosis signaling pathways. However, there are currently few reports on dihydromyricetin's regulation of lipid peroxidation disorders induced by a high-fat diet through the modulation of ferroptosis signaling pathways.

To further confirm the health benefits of vine tea and DMY on a high-fat diet, we established an AS animal model. As we all know, ox-LDL is one of the AS-related risk factors[20-21]. To simulate a daily tea-drinking scenario, we prepared a water extract of vine tea for the experiment. The vine tea extract was obtained through a 4-step process: water extraction, filtration, concentration, and drying, with the content of DMY measuring 40.70%. The pathogenesis of AS generally involves several key processes: immune and inflammatory responses, oxidative stress, and lipid metabolism[22-24]. In addition, a prolonged high-fat diet can lead to impaired liver function, resulting in non-alcoholic fatty liver disease[25]. In this study, after three months of modeling and administration of vine tea water extract, we assessed physiological and biochemical markers associated with AS, such as lipid metabolism-related indicators (TCHO, TG, HDL-C, and LDL-C), inflammation-related markers (IL-6 and TNF-α), and oxidative stress-related markers (LDH, CAT, and GR). Additionally, we monitored indicators related to liver function, including ALT and AST. Our model successfully induced an increase in blood lipid indicators (TCHO, TG, LDL-C), inflammatory cytokines (IL-6 and TNF-α), oxidative stress markers (LDH, CAT, and GR), and liver function indicators (ALT and AST) in the model group compared to the control group (Fig. 3). Furthermore, we employed HE staining and oil red O staining to observe vascular wall damage and lipid deposition across different groups. The data clearly indicate that different doses of vine tea water extract significantly reduced AS-related indicators in rats and decreased lipid deposition in the vascular wall (Fig. 4), suggesting that vine tea has a therapeutic effect on AS rats.

To conduct a comprehensive study on the metabolic changes in rats subjected to a high-fat diet, we employed untargeted metabolomics to identify the differential metabolites in the serum. we conducted KEGG enrichment analysis on differential metabolites and found that vine tea may regulate lipid metabolism, possibly through pathways such as linoleic acid metabolism and glycerophospholipid metabolism (Fig. 5B). As shown in Fig. 5C, after administering vine tea extract, significant downregulation was observed in corresponding lipid metabolites, such as various types of lysophosphatidylcholine (LPC), which are primary phospholipid components of ox-LDL[26-27]. Ox-LDL is also the agent used in our cell model, demonstrating that our experimental design closely aligns with the actual conditions in animals. Thus, we focused on the changes in metabolic indicators related to ferroptosis in the animals. One of the genes associated with ferroptosis is *Nqo1*, and the related metabolite is vitamin K. Following the administration of DMY, transcriptomic data indicated that the *Nqo1* gene was upregulated, whereas metabolomic data demonstrated a decrease in vitamin K levels. Previous studies have confirmed that many vitamin K-dependent proteins contribute to atherogenesis[28], and other prior research has identified the non-canonical vitamin K cycle as a potent suppressor of ferroptosis and lipid peroxidation[29-30]. Another gene related to ferroptosis is *Gclm*, and its associated metabolite is GSH. Interestingly, our metabolomics data revealed no significant changes in GSH levels, both after modeling and following the administration of vine tea water extract. This is because the measurement principle of metabolomics relies on mass spectrometry, which cannot differentiate between the oxidized and reduced forms of GSH. Therefore, we measured T-GSH, GSSG, and GSH in the serum and liver in the AS rats. GSH is a central player in ferroptosis[31-32]. Our results indicated that T-GSH levels did not exhibit significant changes, while GSH levels significantly increased. This finding aligns well with the metabolomics data and transcriptomics results, which showed that *Gclm* expression was upregulated. The detection of ferroptosis-related metabolites in high-fat diet rats further confirms that the effects of vine tea extract and DMY are mediated by the regulation of the ferroptosis signaling pathway.

Although the effects of the water extract of vine tea and its primary component, DMY, on a high-fat diet have been demonstrated, the potential existence of other underlying mechanisms warrants further investigation. Changes in the gut microbiota play a significant role in the onset and progression of diseases. However, this process and its mechanisms cannot be fully elucidated through the cell model. The metabolism of cholesterol and lipids by gut microbiota can influence the development of atherosclerotic plaques[33]. Additionally, diet and specific components metabolized by gut microbiota such as trimethylamine-*N*-oxide can have various effects on AS[34]. In our experimental results, rat fecal 16S rRNA gene sequencing revealed a significant increase in the abundance of Akkermansiaceae within the class Verrucomicrobiae after modeling. Furthermore, following long-term gavage with vine tea extract, the abundance of Lactobacillaceae within the class Bacilli increased (Fig. 6C). Previous studies have reported a lower abundance of the genus *Bacteroides* in patients with coronary artery disease (CAD) compared to those without CAD who possess coronary risk factors, or to healthy voluntears[35]. Our results indicate that the administration of the vine tea extract led to an increased abundance of the genus *Bacteroides*, suggesting a potential therapeutic effect on AS. Additionally, and unexpectedly, our data showed an increased abundance of the family Akkermansiaceae, which is considered beneficial for the progression of AS[28-29], following the high-fat diet modeling. This result is perplexing, as it may be attributed to VD_3 injections. Injecting large doses of VD_3 can increase serum calcium concentration, causing hypercalcemia, which leads to vascular sclerosis and accelerates the formation of AS. However, it may also lead to changes in the gut microbiota, including Lachnospiraceae, Ruminococcaceae, Akkermansiaceae, and Bifidobacteriaceae[36]. Overall, the results after administering vine tea extract are clear. It can alleviate the progression of atherosclerosis by increasing the abundance of family Lactobacillaceae in the gut microbiota. This process may be related to the ability of Bacilli to lower LPC(20:2) and TG(10:0/14:0/i-20:0) levels in the blood (Fig. 6D). Vine tea water extract can increase the abundance of the Lactobacillaceae family in the gut microbiota, thereby reducing lipid metabolites such as LPC in the blood and regulating lipid dysregulation induced by a high-fat diet.

The mechanism by which vine tea exerts its therapeutic effects on high-fat diet-related conditions has become clear (Fig. 8). Its active component, DMY, acts on the ferroptosis pathway and regulates key genes in this pathway, such as *Gclm* and *Nqo1*, thereby increasing GSH levels and modulating the vitamin K cycle. It also increases the abundance of the Lactobacillaceae family in the gut microbiota, leading to a decrease in LPC and TG levels in the blood, thus inhibiting the progression of atherosclerosis induced by high-fat diet.

5. Conclusion

In conclusion, our study provides evidence that vine tea extract can reduce blood levels of TG and other lipids, possesses strong antioxidant properties, and demonstrates effective treatment outcomes in rats fed a high-fat diet. Vine tea achieves these effects by inhibiting the ferroptosis pathway, increasing the abundance of beneficial microorganisms such as Lactobacillaceae in the gut microbiota, and then reducing harmful metabolites like LPC in the blood. Our experimental results provide scientific support for the long-term consumption of vine tea as a preventive measure against atherosclerosis induced by a high-fat diet.

Competing interests

All authors declare that there are no competing interests.

Acknowledgements

The work was supported by Project of Zhangjiajie City's Industry-Academia-Research Collaborative Innovation 'Open Project

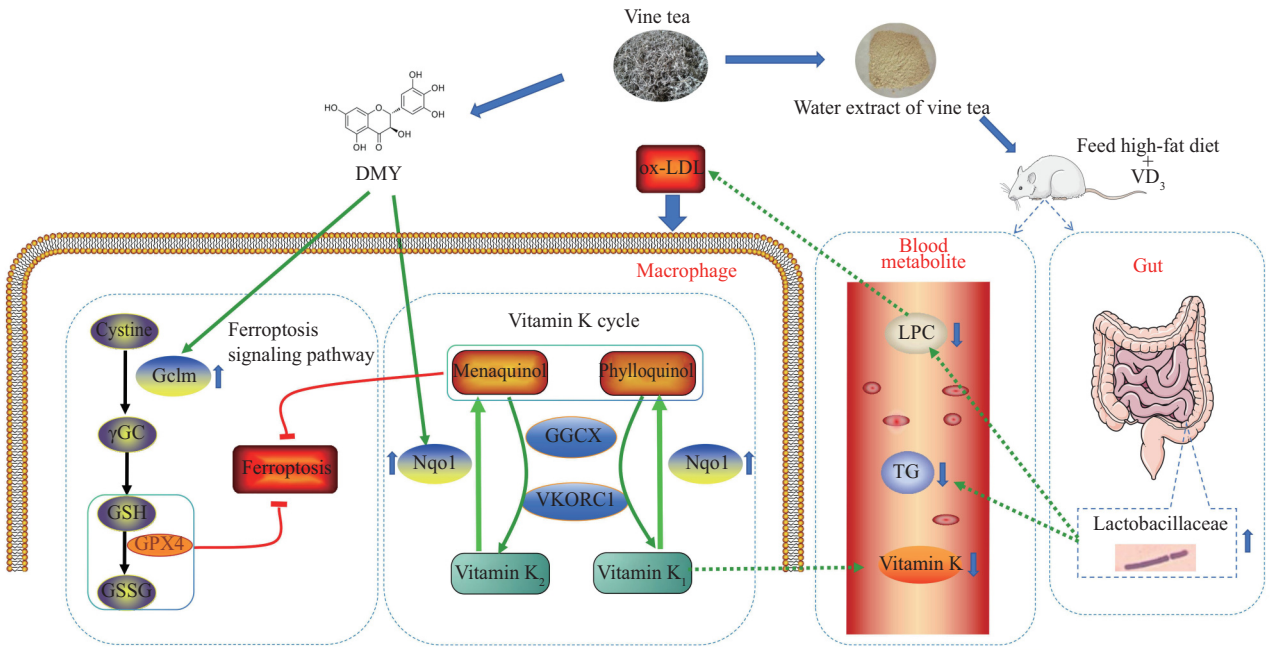

Fig. 8 Mechanism of vine tea extract and its main active component, DYM, in the treatment of a high-fat diet-induced AS rat model. The water extract of vine tea can increase the abundance of Lactobacillaceae in AS model rats, reduce the levels of LPC and TG in serum. Additionally, DYM can regulate the ferroptosis pathway and upregulate key genes involved in this pathway, including *Gclm* and *Nqo1*, which increase GSH levels and modulate the vitamin K cycle, thereby exerting a health-promoting effect. VKORC1, vitamin K epoxide reductase complex subunit 1; GGCX, γ-glutamyl carboxylase.

Leader', Zhangjiajie City's Project of Taking on Challenging Tasks by Responding to Calls for Solutions (JB20230530), Basic Research Funds Project for Central Universities of China (2023XCZX001; 2020kfyXJJS120) and Academician and Expert Workstations in Yunnan Province (202205AF150090).

References

[1] K. Kobiyama, K. Ley, Atherosclerosis A chronic inflammatory disease with an autoimmune component. Circ. Res. 123 (2018) 1118-1120. http://doi.org/10.1161/CIRCRESAHA.118.313816

[2] J.L.M. Björkegren, A.J. Lusis, Atherosclerosis: recent developments. Cell. 185 (2022) 1630-1645. http://doi.org/10.1016/j.cell.2022.04.004.

[3] K. Theodorou, R.A. Boon, Endothelial cell metabolism in atherosclerosis, Front. Cell Dev. Biol. 6 (2018) 82. http://doi.org/10.3389/fcell.2018.00082.

[4] K.J. Moore, F.J. Sheedy, E.A. Fisher, Macrophages in atherosclerosis: a dynamic balance, Nat. Rev. Immunol. 13 (2013) 709-721. http://doi.org/10.1038/nri3520.

[5] Y. Shitara, Y. Sugiyama, Pharmacokinetic and pharmacodynamic alterations of 3-hydroxy-3-methylglutaryl coenzyme A (HMG-CoA) reductase inhibitors: drug-drug interactions and interindividual differences in transporter and metabolic enzyme functions, Pharmacol. Ther. 112 (2006) 71-105. http://doi.org/10.1016/j.pharmthera.2006.03.003.

[6] Y. Luo, S. Lu, X. Dong, et al., Dihydromyricetin protects human umbilical vein endothelial cells from injury through ERK and Akt mediated Nrf2/HO-1 signaling pathway, Apoptosis 22 (2017) 1013-1024. http://doi.org/10.1007/s10495-017-1381-3.

[7] X.Y. Zhang, L.F. Wang, L.Z. Peng, et al., Dihydromyricetin protects HUVECs of oxidative damage induced by sodium nitroprusside through activating PI3K/Akt/FoxO3a signalling pathway, J. Cell. Mol. Med. 23 (2019) 4829-4838. http://doi.org/10.1111/jcmm.14406.

[8] D.F. Yang, S.L. Tan, Z.S. Yang, et al., Dihydromyricetin attenuates TNF-α-induced endothelial dysfunction through miR-21-mediated DDAH1/ADMA/NO signal pathway, Biomed. Res. Int. 2018 (2018) 1047810. http://doi.org/10.1155/2018/1047810.

[9] M.M. Wang, B.D. Cui, M. Gong, et al., *Arctium lappa* leaves based on network pharmacology and experimental validation attenuate atherosclerosis by targeting the AMPK-mediated PPARG/LXRα pathway, Biomed. Pharmacother. 153 (2022) 113503. http://doi.org/10.1016/j.biopha.2022.113503.

[10] Y. Zeng, Y. Peng, K. Tang, et al., Dihydromyricetin ameliorates foam cell formation via LXRα-ABCA1/ABCG1-dependent cholesterol efflux in macrophages, Biomed. Pharmacother. 101 (2018) 543-552. http://doi.org/10.1016/j.biopha.2018.02.124.

[11] L. Zou, Y. Zhang, N. Cheraga, et al., Chlorin e6 (Ce6)-loaded plaque-specific liposome with enhanced photodynamic therapy effect for atherosclerosis treatment, Talanta 265 (2023) 124772. http://doi.org/10.1016/j.talanta.2023.124772.

[12] T.T. Liu, Y. Zeng, K. Tang, et al., Dihydromyricetin ameliorates atherosclerosis in LDL receptor deficient mice, Atherosclerosis 262 (2017) 39-50. http://doi.org/10.1016/j.atherosclerosis.2017.05.003.

[13] X. Chen, J. B. Li, R. Kang, et al., Ferroptosis: machinery and regulation, Autophagy 17 (2021) 2054-2081. http://doi.org/10.1080/15548627.2020.1810918.

[14] B. Hassannia, S. van Coillie, T. Vanden Berghe, Ferroptosis: biological rust of lipid membranes, Antioxid. Redox Signal. 35 (2021) 487-509. http://doi.org/10.1089/ars.2020.8175.

[15] Y.H. Li, G.Y. Shi, Y.L. Han, et al., Therapeutic potential of human umbilical cord mesenchymal stem cells on aortic atherosclerotic plaque in a high-fat diet rabbit model, Stem. Cell Res. Ther. 12 (2021) 407. http://doi.org/10.1186/s13287-021-02490-8.

[16] A. Rzepecka-Stojko, A. Kabala-Dzik, R. Kubina, et al., Protective effect of polyphenol-rich extract from bee pollen in a high-fat diet, Molecules 23 (2018) 805. http://doi.org/10.3390/molecules23040805.

[17] Z.M. Xu, M.J. Zhang, W.W. Wang, et al., Dihydromyricetin attenuates cisplatin-induced acute kidney injury by reducing oxidative stress, inflammation and ferroptosis, Toxicol. Appl. Pharmacol. 473 (2023) 116595. http://doi.org/10.1016/j.taap.2023.116595.

[18] J.B. Xie, T.T. Zhang, P.C. Li, et al., Dihydromyricetin attenuates cerebral ischemia reperfusion injury by inhibiting SPHK1/mTOR signaling and targeting ferroptosis, Drug Des. Dev. Ther. 16 (2022) 3071-3085. http://doi.org/10.2147/DDDT.S378786.

[19] Z.H. Wang, S.D. Feng, Q. Li, et al., Dihydromyricetin alleviates hippocampal ferroptosis in type 2 diabetic cognitive impairment rats via inhibiting the JNK-inflammatory factor pathway, Neurosci. Lett. 812 (2023) 137404. http://doi.org/10.1016/j.neulet.2023.137404.

[20] X. He, X.H. Fan, B. Bai, et al., Pyroptosis is a critical immune-inflammatory response involved in atherosclerosis, Pharmacol. Res. 165 (2021) 105447. http://doi.org/10.1016/j.phrs.2021.105447.

[21] A.J. Kattoor, S.H. Kanuri, J.L. Mehta, Role of ox-LDL and LOX-1 in atherogenesis, Curr. Med. Chem. 26 (2019) 1693-1700. http://doi.org/10.2174/0929867325666180508100950.

[22] R.Y. Wang, M. Wang, J.X. Ye, et al., Mechanism overview and target mining of atherosclerosis: endothelial cell injury in atherosclerosis is regulated by glycolysis, Int. J. Mol. Med. 47 (2021) 65-76. http://doi.org/10.3892/ijmm.2020.4798.

[23] S.E. Engelen, A.J.B. Robinson, Y.X. Zurke, et al., Therapeutic strategies targeting inflammation and immunity in atherosclerosis: how to proceed?, Nat. Rev. Cardiol. 19 (2022) 522-542. http://doi.org/10.1038/s41569-021-00668-4.

[24] U. Förstermann, N. Xia, H.G. Li, Roles of vascular oxidative stress and nitric oxide in the pathogenesis of atherosclerosis, Circ. Res. 120 (2017) 713-735. http://doi.org/10.1161/circresaha.116.309326.

[25] K. Ohashi, Z.J. Wang, Y.M. Yang, et al., NOD-like receptor C4 inflammasome regulates the growth of colon cancer liver metastasis in NAFLD, Hepatology 70 (2019) 1582-1599. http://doi.org/10.1002/hep.30693.

[26] S.H. Law, M.L. Chan, G.K. Marathe, et al., An updated review of lysophosphatidylcholine metabolism in human diseases, Int. J. Mol. Sci. 20 (2019) 1149. http://doi.org/10.3390/ijms20051149.

[27] P.P. Liu, W. Zhu, C. Chen, et al., The mechanisms of lysophosphatidylcholine in the development of diseases, Life Sci. 247 (2020) 117443. http://doi.org/10.1016/j.lfs.2020.117443.

[28] K.L. Berkner, K.W. Runge, The physiology of vitamin K nutriture and vitamin K-dependent protein function in atherosclerosis, J. Thromb. Haemost. 2 (2004) 2118-2132. http://doi.org/10.1111/j.1538-7836.2004.00968.x.

[29] E. Mishima, J. Ito, Z. Wu, et al., A non-canonical vitamin K cycle is a potent ferroptosis suppressor, Nature 608 (2022) 778-783. http://doi.org/10.1038/s41586-022-05022-3.

[30] P. Mladenka, K. Macáková, L.K. Krcmová, et al., Vitamin K: sources, physiological role, kinetics, deficiency, detection, therapeutic use, and toxicity, Nutr. Rev. 80 (2022) 677-698. http://doi.org/10.1093/nutrit/nuab061.

[31] S. Jang, X.R. Chapa-Dubocq, Y.Y. Tyurina, et al., Elucidating the contribution of mitochondrial glutathione to ferroptosis in cardiomyocytes, Redox Biol. 45 (2021) 102021. http://doi.org/10.1016/j.redox.2021.102021.

[32] L.Y. He, Y. Shi, Reduced glutathione ameliorates acute kidney injury by inhibiting ferroptosis, Mol. Med. Rep. 27 (2023) 123. http://doi.org/10.3892/mmr.2023.13011.

[33] A.L. Jonsson, F. Bäckhed, Role of gut microbiota in atherosclerosis, Nat. Rev. Cardiol. 14 (2017) 79-87. http://doi.org/10.1038/nrcardio.2016.183.

[34] B.J.H. Verhaar, A. Prodan, M. Nieuwdorp, et al., Gut microbiota in hypertension and atherosclerosis: a review, Nutrients 12 (2020) 2982. http://doi.org/10.3390/nu12102982.

[35] N. Yoshida, T. Emoto, T. Yamashita, et al., *Bacteroides vulgatus* and *Bacteroides dorei* reduce gut microbial lipopolysaccharide production and inhibit atherosclerosis, Circulation 138 (2018) 2486-2498. http://doi.org/10.1161/CIRCULATIONAHA.118.033714.

[36] S.H. Lee, H.K. Park, C.D. Kang, et al., High dose intramuscular vitamin D_3 supplementation impacts the gut microbiota of patients with clostridioides difficile infection, Front. Cell. Infect. Microbiol. 12 (2022) 904987. https://doi.org/10.3389/fcimb.2022.904987.